Applied Catalysis B: Environmental 119–120 (2012) 256–266

Contents lists available at SciVerse ScienceDirect

Applied Catalysis B: Environmental

journal homepage: www.elsevier.com/locate/apcatb

Selective catalytic reduction of NO_x with methanol over supported silver catalysts

Marika Männikkö*, Magnus Skoglundh, Hanna Härelind Ingelsten

Competence Centre for Catalysis, Department of Chemical and Biological Engineering, Chalmers University of Technology, SE-412 96 Göteborg, Sweden

ARTICLE INFO

Article history:
Received 22 December 2011
Received in revised form 29 February 2012
Accepted 6 March 2012
Available online 14 March 2012

Keywords:
Silver/alumina
Silver/ZSM-5
Methanol-SCR
Lean NO_x reduction
Hydrogen

ABSTRACT

Methanol is a potential renewable fuel for the transport sector and is thus interesting to study as reducing agent for NO_x in hydrocarbon assisted selective catalytic reduction (HC-SCR). The effect of catalyst composition on the lean NO_x reduction during methanol-SCR conditions was investigated. In particular silver supported on alumina and ZSM-5 were in focus and parameters that can improve the NO_x reduction performance, i.e. the C/N molar ratio and the addition of hydrogen, were specifically studied. Five catalysts were prepared (H-ZSM-5, Ag/H-ZSM-5, Pd/Ag/H-ZSM-5, γ-Al_2O_3 and Ag-Al_2O_3) and compared in flow reactor experiments. The Ag-Al_2O_3 (2 wt% Ag, sol–gel) sample was found to give higher NO_x reduction compared to the other tested samples, where important factors are suggested to be the support material, the preparation method and the Ag loading. The NO_x reduction over Ag-Al_2O_3 with methanol is proposed to proceed by adsorbed nitrates or nitrites (or gas phase NO_2) reacting with adsorbed acetate or formaldehyde like species forming adsorbed R—NO_2 or R—ONO, with subsequent conversion into —NCO, —CN, R—NH_2 or NH_3, with final desorption of N_2 and CO_x (or HCHO). The addition of hydrogen and an increase of the supplied methanol concentration resulted in an increased NO_x reduction mainly over the Ag-Al_2O_3 sample, where the addition of hydrogen also extended the active temperature interval towards lower temperatures. Another effect of the addition of hydrogen was formation of more oxidized carbon containing reaction products. The Ag-Al_2O_3 catalyst prepared by the sol–gel method, including freeze-drying of the formed gel, is concluded to be the most promising candidate of the tested catalysts for methanol-SCR.

1. Introduction

Concerns of global climate changes due to increasing anthropogenic CO_2 emissions, promote the development of fuel efficient combustion engines operated in excess oxygen, such as diesel and lean burn engines, as well as the use of biofuels. Dimethyl ether (DME), esters, ethanol and methanol are promising alternative fuels, which can be derived from renewable sources. Methanol is one alternative which presently is discussed as fuel for marine applications. For gasoline engines running under stoichiometric conditions, the three-way catalyst (TWC) is able to simultaneously oxidize CO and hydrocarbons (HC), and reduce nitrogen oxides (NO_x). In presence of excess oxygen, however, its ability to reduce NO_x is severely deteriorated. One available technique to reduce NO_x under lean conditions is selective catalytic reduction using hydrocarbons (HC-SCR), where the (conventional or alternative) fuel is used as the reducing agent, which gives advantages in form of cost, implementation and user-friendliness.

Due to the excess of oxygen in lean combustion the exhaust gas temperature is lower (typically 200–350 °C), than for conventional stoichiometric combustion. Suitable catalysts need to be active in this relatively low temperature region and endure the presence of water vapor and sulfur oxides (SO_x). Metal oxide-based catalysts have been reported to show high stability and moderate resistance to SO_x and water vapor [1]. An example of such a catalyst is Ag supported on alumina, which shows high activity for HC-SCR [1,2]. Also alternative fuels, like ethanol, are reported to give a high NO_x conversion with this technique [3–10]. Using methanol as reducing agent, on the other hand, shows in most studies much lower NO_x conversion with Ag/Al_2O_3 [8–10]. The active temperature region of Ag/Al_2O_3 in methanol-SCR is, however, preferable compared to e.g. γ-Al_2O_3, which is active at higher temperatures [10–12]. A few studies report on remarkably high NO_x conversion with methanol over Ag-Al_2O_3 [13] and over Al_2O_3 [14]. A striking difference in these studies compared to most of the previously mentioned ones is a low flow rate and for the latter also a high C/N ratio. It is, however, difficult to compare results from different studies since there are many parameters influencing the NO_x reduction performance; as the active metal loading [15], the catalyst preparation method [16] and the experimental conditions, e.g. the amount of catalyst used, the feed composition and the flow rate [17]. The study by

* Corresponding author. Tel.: +46 31 7722938; fax: +46 31 160062.
E-mail address: marika.mannikko@chalmers.se (M. Männikkö).

0926-3373/$ – see front matter © 2012 Elsevier B.V. All rights reserved.
doi:10.1016/j.apcatb.2012.03.006

Miyadera [8] was one of the first to show high NO_x conversion over Ag/Al_2O_3 by ethanol. The authors reported higher activity over Ag/Al_2O_3, compared to Al_2O_3 and Co/Al_2O_3, when water was present in the feed. Kameoka et al. [10] found that the addition of Ag to Al_2O_3 resulted in lower NO_x reduction by methanol and suggested that this could be due to Ag enhancing the total oxidation of methanol. A reaction mechanism for alcohols and hydrocarbons was proposed, with intermediates including adsorbed nitrates, partially oxidized hydrocarbons and isocyanate species. Wu et al. [9] suggested a reaction mechanism for ethanol-SCR, where a high concentration of surface isocyanate species promotes an efficient NO_x reduction. However, methanol-SCR was concluded not to follow the same reaction path and a few years later the research group suggested a reaction mechanism for C1 reductants, with intermediates including formates and nitrates. These surface species have low reactivity in forming —NCO species, resulting in low NO_x reduction [18]. Tamm et al. [19] studied the evolution of surface species in DME-SCR and methanol-SCR over γ-Al_2O_3 and found, besides the previously mentioned formates, nitrates and —NCO species, also e.g. formaldehyde-like species. The reaction mechanism was proposed to be similar to the one previously suggested for HC-SCR over Ag/Al_2O_3 by Tamm et al. [20], involving two parallel pathways for —NCO and —CN species. Masuda et al. [12] concluded that methanol is a suitable reducing agent for NO_x over Ag/Al_2O_3 at relatively high temperatures, while Ag/mordenite and Ag-ZSM-5, showed poor NO_x reduction with methanol. On the other hand, when DME (which is known to behave similarly to methanol) was used as reducing agent Ag/mordenite, was suggested as a possible catalyst for NO_x removal from automotive sources. Later, improved NO_x reduction was reported for DME as reductant over Ag(3%)/mordenite impregnated with a small amount of Pd (0.01%) [21]. These experiments were performed at high space velocity, and it was found that a high amount of acid sites is beneficial for the NO_x conversion.

The objective of the present work is to investigate the selective catalytic reduction of NO_x under lean conditions using methanol as the reducing agent. In particular silver supported on alumina and ZSM-5 are in focus and parameters that can improve the NO_x reduction performance, i.e. the C/N molar ratio and the addition of hydrogen are specifically studied. The results are discussed in relation to possible reaction pathways.

2. Experimental methods

2.1. Catalyst preparation

Five monolith catalyst samples were prepared and used in this work, i.e. H-ZSM-5, Ag/H-ZSM-5, Pd/Ag/H-ZSM-5, γ-Al_2O_3 and Ag-Al_2O_3. Zeolite H-ZSM-5 powder (Akzo Nobel Catalysts BV) with a SiO_2/Al_2O_3 molar ratio of 40 was used as received for the preparation of a H-ZSM-5 coated monolith catalyst. Detailed properties of the zeolite are found elsewhere [22]. The H-ZSM-5 powder was also used to prepare Ag/H-ZSM-5 through ion-exchange. Part of the prepared Ag/H-ZSM-5 sample was subsequently used to prepare Pd/Ag/H-ZSM-5 by incipient wetness impregnation. First, the zeolite was calcined in air (550 °C for 2 h). The silver ion-exchange was conducted by adding 12 g zeolite to a 300 ml 0.01 M $AgNO_3$ (Rectapur) solution (Milli-Q water), adjusted to approximately pH 7 with diluted NH_4OH and stirred at room temperature for 21 h. Finally the water was removed after centrifugation. The ion-exchange procedure was then repeated and the sample was washed three times with Milli-Q water and freeze dried. The preparation was carried out in the dark. Pd/Ag/H-ZSM-5 was prepared through incipient wetness impregnation by mixing 3 g of the dried Ag/H-ZSM-5 sample with a $Pd(NO_3)_2$-solution (Johnson Matthey). The slurry was stirred for 15 min and freeze dried. The amount of $Pd(NO_3)_2$-solution used corresponded to a palladium content of 0.01 wt% in the dry powder sample. Both the Ag/H-ZSM-5 and the Pd/Ag/H-ZSM-5 samples were calcined in air (550 °C for 2 h). A γ-Al_2O_3 powder (Sasol, Puralox SBa200) was used as received in the preparation of an Al_2O_3 coated monolith catalyst. Ag-Al_2O_3 was prepared according to the sol–gel method including freeze-drying, described by Kannisto et al. [16]. A sol was formed by slowly adding diluted nitric acid to an aqueous solution of aluminum isopropoxide (AIP) and $AgNO_3$. Removal of excess solvent resulted in a gel, which was freeze-dried, crushed and finally calcined in air (600 °C for 6 h). The silver loading corresponded to 2 wt%.

For the flow reactor experiments the powder samples were deposited on cordierite monolith substrates (Corning, 400 cpsi, 188 channels). The monoliths (diameter 20 mm) were cut from a 20 mm thick block and calcined in air at 600 °C for 20 min. For each catalyst a slurry was prepared by mixing the powder sample and a binder at a weight ratio of 80:20 in Milli-Q water. The binders used were Bindzil (30NH_3/220, Colloidal Silica, Akzo Nobel, Eka Chemicals) and Disperal P2 (Sasol) for the ZSM-5 and γ-Al_2O_3 catalysts, respectively. The monoliths were immersed in the wash-coat slurry, dried (90 °C, 5 min) and calcined (550 °C, 2 min). The procedure was repeated until the weight of the wash-coat was 20% of the final dry monolith sample weight. The monolith samples were finally calcined in air at 550 °C for 2 h and at 600 °C for 2 h and 3 h, for the zeolite based, Al_2O_3 and Ag-Al_2O_3 samples, respectively.

2.2. Sample characterization

2.2.1. Ag content

The resulting silver content in the Ag/H-ZSM-5 and Pd/Ag/H-ZSM-5 powder samples was analyzed by SEM-EDX (Leo Ultra 55 FEG SEM, Oxford Inca EDX system) and found to be 5 wt%, which corresponds to 60% exchange of the hydrogen ions by silver ions. Since the nominal content of Pd was very low (0.01 wt%) in the Pd/Ag/H-ZSM-5 sample, the Pd content was not possible to analyze.

2.2.2. Specific surface area

The BET method [23] was used to determine the specific surface area of the samples, using a Micromeritics Tristar 3000 for the powder samples and a Micromeritics ASAP 2010 for the monolith samples. Fresh powder samples, as well as both fresh and used monolith samples were analyzed. The used monolith samples were analyzed after methanol-SCR and NH_3-TPD experiments in the flow reactor described below.

2.2.3. Surface acidity

Temperature programmed desorption (TPD) of ammonia was performed in a flow reactor, described below, in order to determine the surface acidity of the monolith samples. Before adsorption of ammonia, the sample was pretreated at 500 °C in 10% O_2 in Ar (20 min), flushed with Ar (5 min), and finally in 0.5% H_2 in Ar (20 min). The sample was subsequently cooled to 100 °C in Ar and exposed to ammonia until saturation (1000 ppm NH_3 in Ar, 100 °C, 45 min). The sample was then flushed with Ar for 1 h in order to remove weakly bound ammonia, and the final desorption was carried out in Ar (10 °C/min, 100–500 °C).

2.2.4. Silver species

UV–vis diffuse reflectance spectroscopy was performed to characterize silver species. Spectra, in the range 200–1500 nm, were recorded for the powder samples (H-ZSM-5, Ag/H-ZSM-5, γ-Al_2O_3 and Ag-Al_2O_3) in air at room temperature, using a Varian Cary

Table 1
Specific surface area of the prepared powder and monolith samples. The specific surface area of the monolith samples (containing 0.5 g wash-coat) was measured both before and after the flow reactor experiments.

BET surface area	ZSM-5 based samples			Al_2O_3 based samples	
	H-	Ag-	Pd/Ag-	γ-	Ag-
Powder (m^2/g)	403	364	316	194	176
Monolith-fresh (m^2/monolith)	181	165	158	95	–
Monolith-used (m^2/monolith)	177	154	155	91	71

5000 UV–vis–NIR spectrophotometer, with Labsphere Spectralon as reference.

2.3. Catalytic performance

The catalytic performance with respect to lean NO_x reduction with methanol was studied in a continuous flow reactor consisting of a horizontally mounted quartz-tube in which the monolith sample was placed. Before and after the monolith sample an uncoated cordierite monolith was placed in order to minimize temperature and flow gradients, as described by Wang-Hansen et al. [24]. The inlet gas and sample temperatures were measured inside one of the channels in the center of the uncoated monolith preceding the sample monolith and inside a channel in the center of the sample monolith, respectively. Feed gases (Ar, O_2, NO, NH_3, H_2) were introduced into the reactor via separate mass flow controllers (Bronkhorst Hi-Tech). Methanol was introduced to the reactor via a CEM-system (controlled evaporator mixer; Bronkhorst Hi-Tech); where the methanol and carrier gas (Ar) flows were controlled by mass flow controllers (Bronkhorst Hi-Tech). The outlet gas composition was analyzed by a gas phase FTIR analyzer (MKS Instruments, MultiGas 2030).

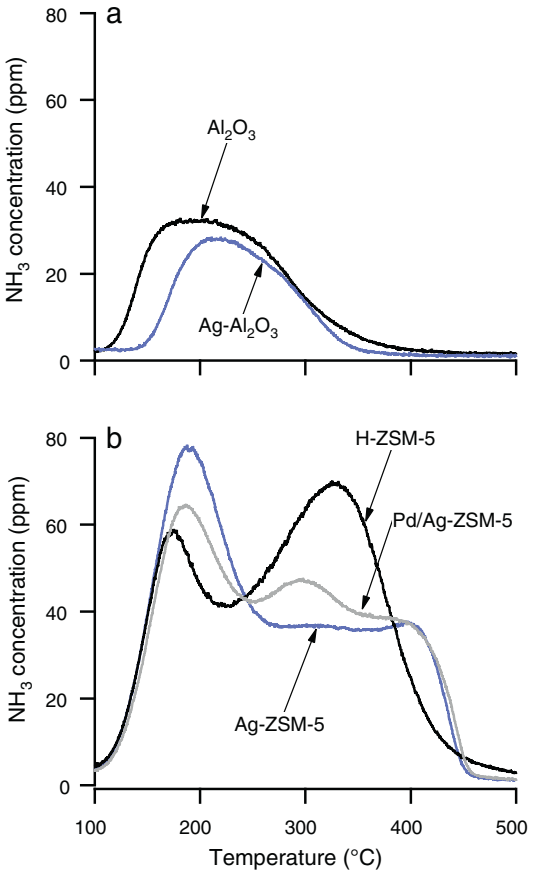

Fig. 1. NH_3-TPD for alumina based (a) and ZSM-5 based (b) samples. The samples were exposed to 1000 ppm NH_3 until saturation at 100 °C. After flushing with Ar for 1 h, desorption was carried out in Ar (10 °C/min, 100–500 °C).

In order to compare the catalytic activity of the samples several experiments were performed. Before each experiment the catalyst was pretreated in 10% O_2 in Ar at 550 °C for 30 min and then flushed with Ar for 15 min. Temperature programmed reaction experiments (400–150 °C, 5 °C/min) were performed with a feed gas composition of 500 ppm NO, 850 ppm methanol and 10% O_2, balanced with Ar. For the silver containing catalysts the experiment was repeated with addition of 1000 ppm H_2 to the feed gas, keeping the total gas flow constant by balancing with Ar. Steady state experiments were performed at 350 °C with a feed gas composition of 500 ppm NO, 10% O_2 and varying concentrations of methanol, giving C/N molar ratios of 0, 1.7, 3.4, 5.1 and 6.8. In addition to the pretreatment in 10% O_2 at 550 °C the steady state experiments were preceded by a conditioning step of 500 ppm NO, 1000 ppm methanol and 10% O_2, balanced in Ar, at 350 °C for 1 h, followed by 30 min of Ar exposure at the same temperature. All flow reactor experiments were performed using a total flow of 3500 ml/min, corresponding to a space velocity (GHSV) of 33,400 h^{-1}. The conversion of NO_x to N_2 was calculated from the concentrations of nitrogen containing species detected by the gas phase FTIR in the following way. The total concentration (in molar ppm of N atoms) of all detected nitrogen containing species (i.e. NO, NO_2, N_2O, NH_3 and HCN) in the outlet from the reactor was subtracted from the inlet concentration of NO (500 ppm), and divided by the inlet concentration of NO. This will include any adsorbed nitrogen into the calculated amount of N_2. However, comparisons with heating ramp experiments show that the adsorption of nitrogen is negligible in the temperature region for the NO_x conversion to N_2. Thus, the amount of nitrogen that cannot be detected by FTIR in the outlet gas stream is assumed to be in the form of N_2. The conversion of methanol was calculated by subtracting the detected methanol concentration from the inlet concentration (850 ppm) and dividing it by the inlet concentration. In the high temperature region the sum of carbon containing species does not completely match the calculated methanol conversion in all presented experiments due to difficulties in calibrating CO and CO_2, and due to the fact that formaldehyde was not calibrated. Species present in low amounts (acetaldehyde, CH_4, HCN, NH_3, N_2O) were not calibrated, since tests with gases at low concentrations have shown that the values shown by the FTIR analyzer have a good accuracy below ca. 100 ppm.

3. Results

3.1. Characterization

3.1.1. Specific surface area

The results from the specific surface area measurements are summarized in Table 1. As expected the zeolite samples show a higher BET surface area than the Al_2O_3 samples. The high specific surface area of the H-ZSM-5 sample decreased after Ag ion-exchange and Pd impregnation. All samples show a minor decrease in specific surface area after the flow reactor experiments (<10%). Since this decrease is not extensive the monolith samples can

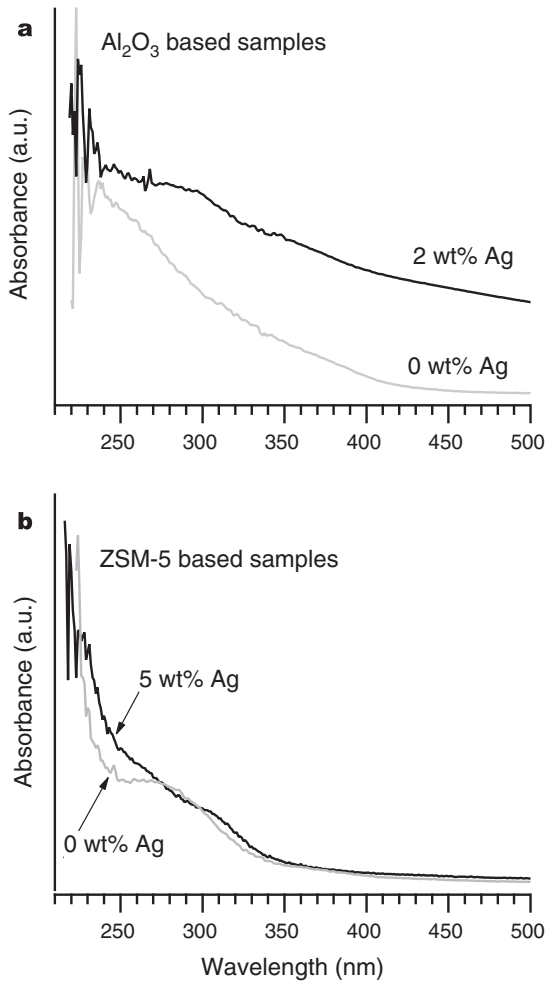

Fig. 2. UV–vis spectra (a) of the Ag-Al_2O_3 and γ-Al_2O_3 samples, and (b) of the Ag-ZSM-5 and H-ZSM-5 samples.

be expected to show comparable results throughout the series of experiments performed in this study.

3.1.2. NH_3-TPD

The results from the NH_3 temperature programmed desorption experiments for the tested catalysts are shown in Fig. 1. The alumina based samples show a peak around 200 °C, with a shoulder at higher temperature. The peak for the Ag-Al_2O_3 sample is slightly shifted to higher temperature and is somewhat lower compared to the Al_2O_3 sample. Thus, the Ag-Al_2O_3 sample has a lower number of weak acid sites than the Al_2O_3 sample. The zeolite based samples show three peaks around 200 °C, 300 °C, and 400 °C, which are assigned to weakly bound NH_3, Brønsted acid sites and Lewis acid sites created by the metal cations [25–27].

3.1.3. Silver species

The silver species in the Ag-ZSM-5 and Ag-Al_2O_3 samples were characterized with UV–vis spectroscopy, and compared with the spectra of the H-ZSM-5 and γ-Al_2O_3 samples. The UV–vis spectra are shown in Fig. 2. Peaks are observed in the regions 230–260 nm and 310–330 nm for the Ag-ZSM-5 sample, while the Ag-Al_2O_3 sample shows absorption peaks in the region 215–240 nm, and at ca. 300 and 350 nm.

3.2. Activity for lean NO_x reduction

The conversion of NO and methanol was studied in flow reactor experiments during cooling ramps in oxygen excess and the results are shown in Fig. 3. The Al_2O_3 and H-ZSM-5 samples show the highest NO_x reduction in the high temperature region of Fig. 3a, while the Ag-Al_2O_3 sample shows the best NO_x reduction performance at lower temperatures (below ca. 360 °C). The NO_x conversion over the Ag-ZSM-5 and Pd/Ag-ZSM-5 samples is low (below 5%). Fig. 3b shows that the conversion of methanol over all the tested catalysts increases with increasing temperature, and reaches 90–100% at 400 °C. In all cases the methanol conversion starts at a lower temperature than the NO_x conversion. Fig. 3c–f shows the formation of products formed from NO and methanol in oxygen excess over the tested catalysts as a function of the inlet temperature. DME is formed at lower temperatures, while mainly CO, CO_2 and formaldehyde are formed at higher temperatures.

For the Ag-Al_2O_3 sample the NO_x conversion to N_2 shows a maximum of 18% at ca. 330 °C (C/N ratio = 1.7), shown in Fig. 3c. The sum of NH_3, HCN and N_2O gives a maximum of 6% of the NO inlet at 300 °C. Fig. 3c shows that methanol is converted to several carbon containing species over the Ag-Al_2O_3 sample: CO_2, CO, DME, formaldehyde, HCN, methane and acetaldehyde, where the concentration of the last two compounds is below 10 ppm. These results show resemblances with previous methanol-TPO [19,28,29] and SCR experiments [11]. The maximum formation of NH_3, DME, HCHO and CH_3CHO over the Ag-Al_2O_3 sample can be observed around 280 °C. The corresponding temperature for HCN and CH_4 is 300 °C. When approaching 400 °C the formation of CO increases while the formation of CO_2 seems to be close to its maximum. Formation of all species over the Al_2O_3 sample, except DME, are shifted towards higher temperatures (above 250 °C) compared to the Ag-Al_2O_3 sample. The NO_x conversion over the Al_2O_3 sample starts around 320 °C, where the formation of all other species, besides DME, also starts. The highest conversion of NO_x to N_2 over the Al_2O_3 sample in the tested temperature interval is 25% at 400 °C (Fig. 3a). Tamm et al. [11] found a maximum NO_x conversion around 450 °C for methanol-SCR over Al_2O_3. The selectivity towards N_2 is higher over the Al_2O_3 sample compared to the Ag-Al_2O_3 sample, which is in agreement with the results by Tamm et al. [11]. A maximum of 2% of inlet NO is converted to NH_3, HCN and N_2O at 360 °C. As over the Ag-Al_2O_3 sample the maximum formation of NH_3 and formaldehyde coincide (at ca. 360 °C) over the Al_2O_3 sample. Unlike over the Ag-Al_2O_3 sample, the formation of CO is considerably more extensive than the formation of CO_2 over the Al_2O_3 sample, in agreement with previous studies [11,29,30]. Another significant difference compared to the Ag-Al_2O_3 sample is the formation of DME, which is more extensive and occurs during a broader temperature interval over the Al_2O_3 sample. The methanol conversion over the Al_2O_3 sample increases in two steps with increasing temperature, which also has been observed previously [11,14]. At lower temperatures DME is the main reaction product and at higher temperatures CO, CO_2, formaldehyde and small amounts of CH_4 are formed.

Fig. 3a and b shows that the conversion of NO_x and methanol over H-ZSM-5 follow a similar trend as over Al_2O_3. The NO_x conversion to N_2 continues to increase over H-ZSM-5 when approaching 400 °C and reaches about the same level (25%) as over Al_2O_3. Tamm et al. [31] also showed an increasing NO_x conversion over H-ZSM-5 (SAR 40) with increasing temperature in DME-SCR in the absence of water. However, the NO_x conversion seen by Tamm et al. [31] only reached ca. 10% at 400 °C with C/N ratio = 2. The H-ZSM-5 sample shows the highest formation of HCN (24 ppm at 400 °C) among the tested catalysts. Together with N_2O this corresponds to 7% of the inlet NO. Compared to the Al_2O_3 sample, the H-ZSM-5 sample shows a higher formation of formaldehyde, a lower formation of

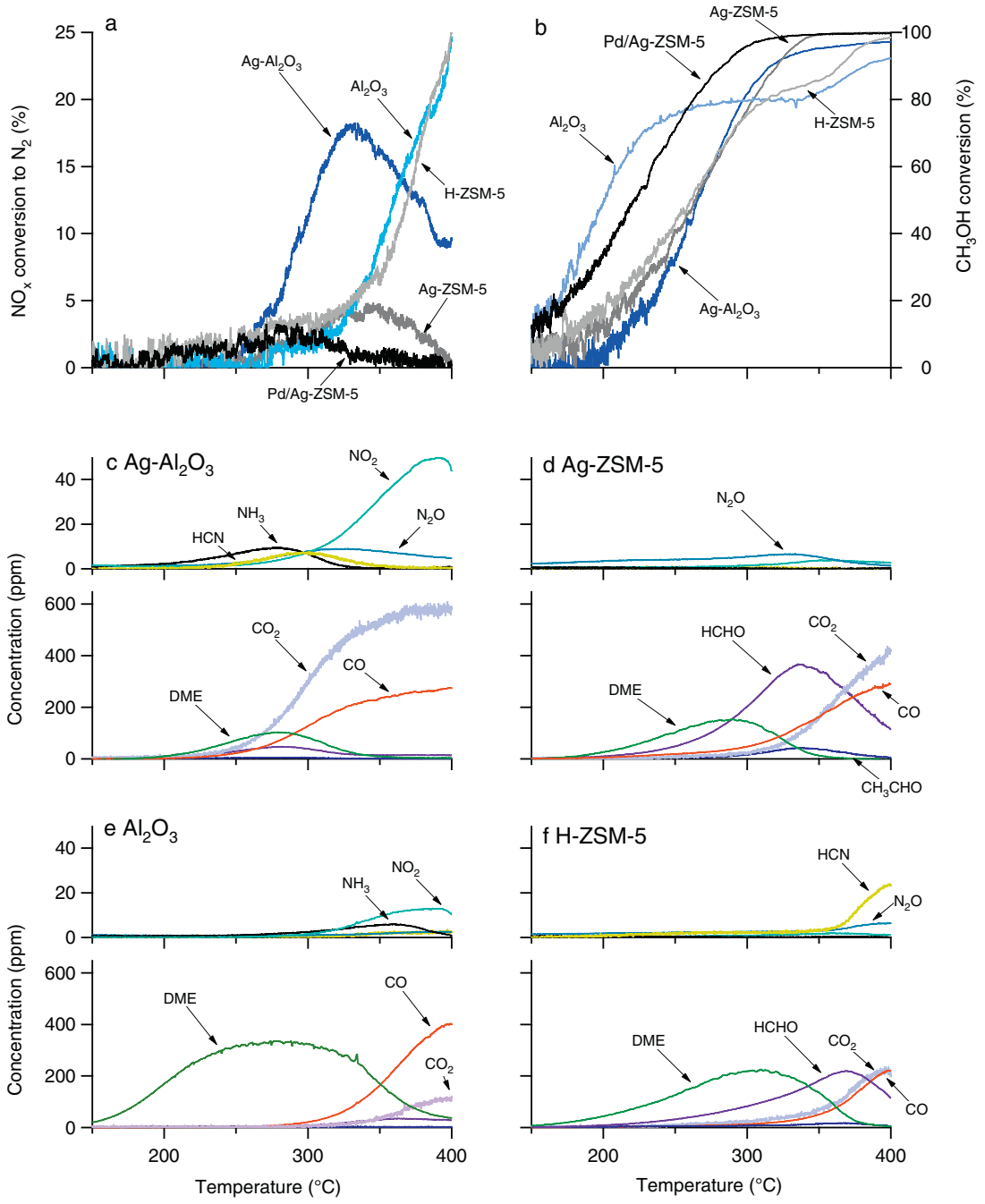

Fig. 3. NO_x conversion (a) and methanol conversion (b) over the Al_2O_3, Ag-Al_2O_3, H-ZSM-5, Ag-ZSM-5 and Pd/Ag-ZSM-5 catalyst samples, and conversion products formed over the (c) Ag-Al_2O_3, (d) Ag-ZSM-5, (e) Al_2O_3 and (f) H-ZSM-5 catalyst samples, during cooling ramps in 850 ppm CH_3OH, 500 ppm NO and 10% O_2, balanced in Ar. The upper parts of c–f show the nitrogen containing reaction products, and the lower parts show the carbon containing reaction products.

CO and NO_2 and a negligible formation of NH_3 and CH_4, which is in accordance with the results for the other two zeolite based catalysts. Another difference compared to the Al_2O_3 sample is the less pronounced formation of DME over H-ZSM-5. Fig. 3a shows that the maximum NO_x conversion over the Ag-ZSM-5 sample (at 340 °C) is much lower (below 5%) than over the Ag-Al_2O_3 sample, in agreement with the studies by Masuda et al. [12] and Tamm et al. [31]. As much as 3% of the inlet NO is converted to (mainly) N_2O, resulting in a low selectivity to N_2 (Fig. 3d). There is a significant shift towards higher temperatures in the formation of CO_2, CO, formaldehyde and acetaldehyde over the Ag-ZSM-5 sample, while the formation of DME is only slightly shifted towards higher temperatures, compared to the Ag-Al_2O_3 sample. For all tested ZSM-5 based samples, the formation of formaldehyde is significantly higher (a maximum of ca. 370 ppm over Ag-ZSM-5), compared to the alumina based samples. The Pd/Ag-ZSM-5 sample shows similar results as the Ag-ZSM-5 sample, except that the formation of all detected species is shifted towards lower temperatures and that the NO_x reduction (shown in Fig. 3a) is even lower, below 3%.

3.3. *Influence of hydrogen on the NO_x reduction*

The influence of H_2 on the conversion of NO over the Ag containing catalyst samples was studied in flow reactor experiments during cooling ramps in oxygen excess. When 1000 ppm H_2 is added to the feed the conversion of both NO_x and methanol shift

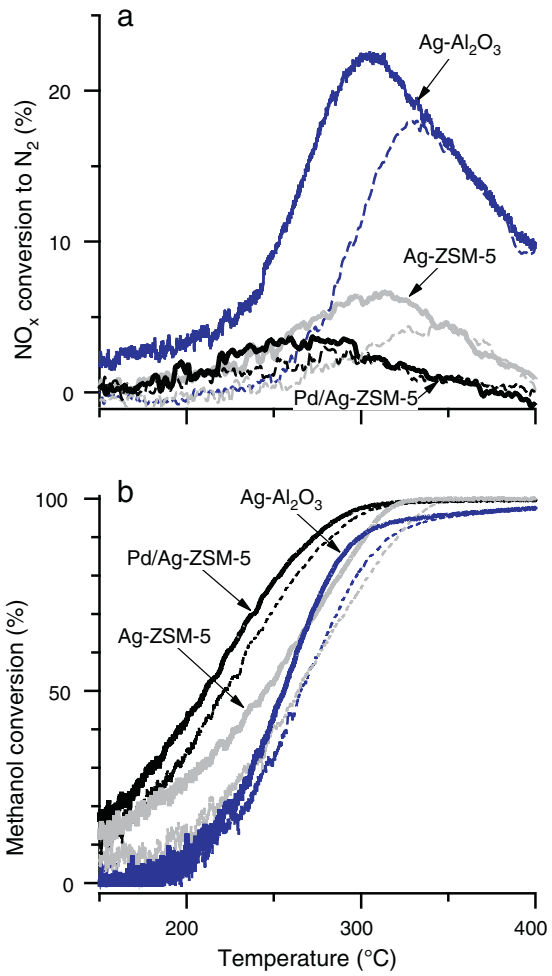

Fig. 4. Influence of H_2 on the NO_x conversion (a) and the methanol conversion (b) over the Ag-Al_2O_3, Ag-ZSM-5 and Pd/Ag-ZSM-5 catalyst samples. Temperature ramps during cooling in a gas mixture of 850 ppm CH_3OH, 500 ppm NO and 10% O_2, with 1000 ppm H_2 (bold lines) and without H_2 (dotted lines), balanced in Ar.

towards lower temperatures for all the tested catalysts, as shown in Fig. 4. The same trend applies for the formation of all other detected species (shown for Ag-Al_2O_3 in Fig. 5). The largest positive effect on the NO_x conversion is seen over the Ag-Al_2O_3 sample, while the NO_x reduction over the two ZSM-5 based samples remains low even in the presence of H_2. The conversion of NO_x to N_2 over the Ag-Al_2O_3 sample in the presence of hydrogen shows a maximum of 22% at ca. 305 °C (Fig. 4), and the addition of H_2 enhances the NO_x conversion in the temperature region 220–330 °C. The methanol conversion over the Ag-Al_2O_3 sample starts at about the same temperature as without H_2 but increases more rapidly, before it levels out after the maximum NO_x conversion and reaches the same level as without H_2. Fig. 5 shows that the addition of H_2 results in a more extensive formation of in particular CO_2, N_2, NO_2 and N_2O, while the DME formation decreases. The carbon containing products formed over Ag-Al_2O_3 are oxidized to a higher extent when hydrogen is present in the feed. This is illustrated in the bottom panel of Fig. 5, showing the weighted sum of the oxidation state of carbon for the detected carbon containing (gas phase) products. For each carbon containing product (CO_2, CO, HCN, HCHO, DME) the oxidation state was multiplied with the yield (=concentration of the carbon product divided by the inlet concentration of methanol), where after the sum of the products was calculated. The oxidation state used for carbon in CO_2, CO, HCN, HCHO and DME, was +4, +2, +2, 0 and −2, respectively. The bottom panel of Fig. 5 shows that the weighted oxidation state

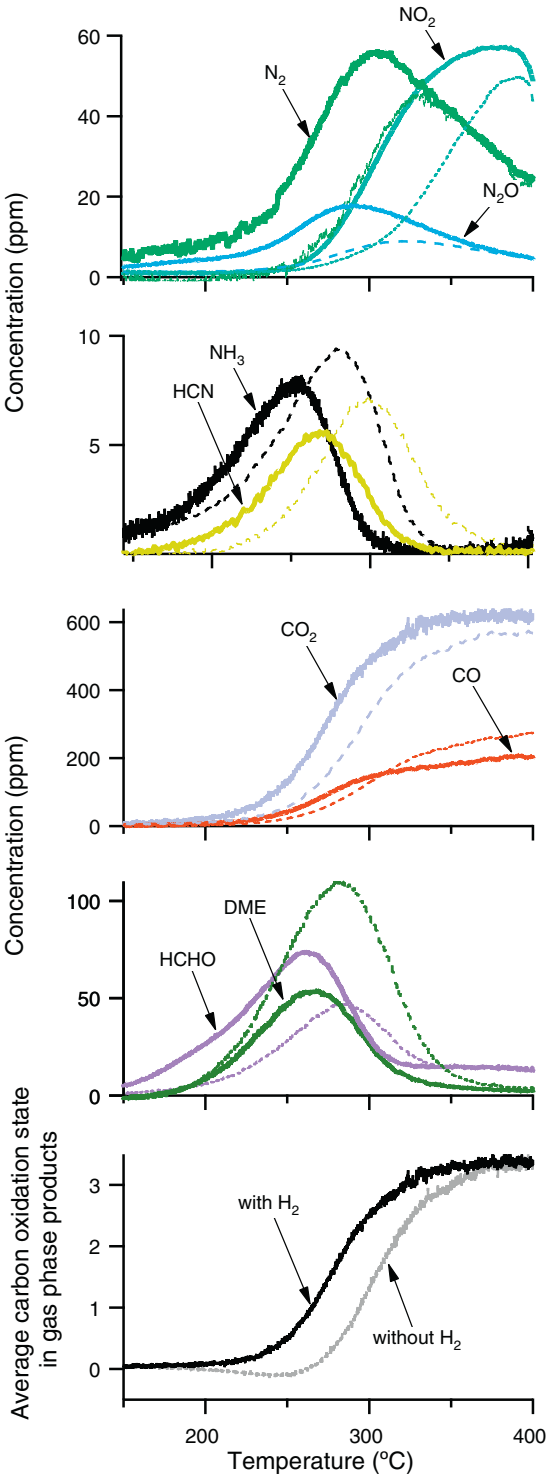

Fig. 5. Influence of H_2 on the catalytic performance of the Ag-Al_2O_3 sample. Temperature ramps during cooling in a gas mixture of 850 ppm CH_3OH, 500 ppm NO and 10% O_2, with 1000 ppm H_2 (solid lines) and without H_2 (dotted lines), balanced in Ar. The N_2 concentration is calculated from the detected nitrogen containing species. The average oxidation number of carbon in products (bottom panel) was calculated from the sum of the products of oxidation number of C and yield, for each carbon containing product (CO_2, CO, HCN, HCHO, DME).

of carbon for the carbon containing products formed over Ag-Al_2O_3 always is higher when hydrogen is added to the feed, compared to when no hydrogen is present in the temperature interval where NO_x is reduced. The conversion of NO_x to N_2 over the Ag-ZSM-5 sample increases slightly in the presence of H_2, while the effect is negligible over the Pd/Ag-ZSM-5 sample (Fig. 4). For both catalysts

the addition of H_2 gives a somewhat higher formation of CO_2 and N_2O.

3.4. Influence of C/N molar ratio on the NO_x reduction

The conversion of NO and methanol in oxygen excess was studied at constant temperature (350 °C), while varying the C/N molar ratio. The C/N molar ratio is increased every 30 min and the results are shown in Fig. 6. The outlet gas concentrations in this experiment (Fig. 6) show similarities with those in the cooling ramp experiments (Fig. 3).

Increasing the C/N molar ratio results in a significant increase in the NO_x conversion to N_2 over the Ag-Al_2O_3 sample, while for the other catalysts only a small or negligible increase in NO_x reduction can be observed (Fig. 6). For the Ag-Al_2O_3 sample C/N ratios of 1.7, 3.4, 5.1 and 6.8 results in 15, 28, 39 and 48% NO_x conversion to N_2, respectively. The concentration of almost all detected species increases with increasing C/N molar ratio. The only exception, besides NO, is NO_2 which decreases when the C/N molar ratio is increased from 5.1 to 6.8 over Ag-Al_2O_3 (Fig. 6). The increase of each carbon species formed over the Ag-Al_2O_3 sample is proportional to the increase of the methanol concentration in the feed. The positive effect on the NO_x reduction over the Al_2O_3 sample is weaker than over the Ag-Al_2O_3 sample when the C/N molar ratio is increased at 350 °C. Fig. 6 shows that all the detected species, except NO, increase in concentration when the C/N molar ratio is increased over Al_2O_3. This effect is mostly pronounced for DME and NO_2, where the NO_2 increase is higher in each methanol step.

Fig. 6 shows that increasing the C/N molar ratio has negligible effect on the NO_x conversion to N_2 over the zeolite based catalysts. A general remark for the ZSM-5 based catalysts is that the stabilization of the outlet gas concentrations after a change in feed gas composition requires longer time compared to the alumina based catalysts. Most of the species detected in significant amounts (higher than 5 ppm) over the ZSM-5 samples increase in concentration with increasing C/N ratio. The most abundant carbon species at the high C/N molar ratios are methanol, formaldehyde and CO_2 over the H-ZSM-5, Ag-ZSM-5 and Pd/Ag-ZSM-5 samples, respectively. When only NO and O_2 is present in the gas feed, a larger part of the NO fed into the reactor is converted to NO_2 over the zeolite based catalysts than over the alumina based catalysts, as shown in Fig. 6. Thus, ZSM-5 seems to promote the NO oxidation more than Al_2O_3. The H-ZSM-5 sample shows the lowest conversion of methanol of all the tested catalysts at 350 °C. In fact the conversion of methanol decreases, when the C/N ratio increases (Fig. 6).

4. Discussion

4.1. Surface acidity and specific surface area

A high number of acidic sites is reported to be beneficial for HC-SCR for several reducing agents, e.g. with DME (which is known to behave similarly to methanol) over both ZSM-5 [31] and γ-Al_2O_3 [29]. The NH_3-TPD experiments in Fig. 1 show a higher peak area for the Al_2O_3 sample at low temperature (ca. 150–200 °C), compared to the Ag-Al_2O_3 sample. Thus, the Al_2O_3 sample has a higher number of weak acid sites than the Ag-Al_2O_3 sample. The Ag-Al_2O_3 sample shows a shoulder at higher temperature (ca. 300 °C). To which extent the active sites represented by this shoulder are present also in the Al_2O_3 sample is not obvious from these results. For the ZSM-5 based samples the desorption peak at low temperature (ca. 200 °C) in the NH_3-TPD experiments has been reported as weakly bound NH_3 [25]. The peak around or just above 300 °C, is commonly assigned to Brønsted acid sites [25,26]. The shift in temperature for this peak between H-ZSM-5 and the Ag exchanged ZSM-5 samples corresponds to results in other studies [12,27]. The high-temperature peak around 400 °C in the Ag exchanged ZSM-5 samples corresponds to the desorption peak observed by Lersch and Bandermann [27] in other cation exchanged ZSM-5 catalysts, which has been assigned to Lewis acid sites created by the metal cations. Interestingly, despite a lower number of acidic sites and a lower specific surface area (Table 1), the Ag-Al_2O_3 sample shows higher NO_x reduction with methanol (Fig. 3), compared to the Ag containing ZSM-5 samples. The NO_x reduction performance of H-ZSM-5 is, however, comparable to Al_2O_3 in the investigated temperature interval. For the Ag containing catalysts it can be concluded that other parameters, than the acidity and specific surface area, are more important in order to achieve high NO_x reduction in methanol-SCR. Below we discuss the importance of Ag loading and the nature of the Ag sites.

4.2. Dispersion and chemical state of silver

Small oxidized Ag clusters or ions are believed to be beneficial for NO_x reduction to N_2. Such small oxidized silver clusters or ions are thought to be present in high amounts in Ag-Al_2O_3 prepared by the sol–gel method [16], where freeze-drying results in more highly dispersed Ag than thermal drying. Zhu et al. [13] studied Ag-Al_2O_3 prepared by the sol–gel method, where the maximum NO_x reduction with methanol was found to be at the same level as when ethanol was used as reductant, even though the C/N molar ratio for methanol was lower than for ethanol. These results are surprising compared to other studies where ethanol was found to give a higher NO_x reduction than methanol over Ag/Al_2O_3, where the samples were prepared by conventional impregnation [8–10]. Ag/Al_2O_3 prepared by the conventional impregnation technique, was reported by Kannisto et al. [16] to contain a higher degree of metallic Ag, which is known to promote combustion of hydrocarbons. Also high loadings of silver were found by Bethke and Kung [32] to promote the metallic form of silver, enhancing combustion of the reducing agent. At lower loadings, Ag is reported to be present in an oxidized form, which is beneficial for NO_x reduction to N_2 [32]. Thus, both the Ag loading and the preparation method influence the resulting state of silver in the final catalyst, and consequently also the NO_x reduction performance. In the case of methanol-SCR a sample with low Ag loading prepared by the sol–gel method using freeze-drying should be beneficial. This is a possible reason to why the Ag-Al_2O_3 (2 wt% Ag) sample in this study was found to give high NO_x reduction. The Ag-ZSM-5 sample was prepared by ion-exchange, where Ag^+ ions replace H^+ ions in the zeolite, also expected to result in high dispersion of silver. Meunier et al. [33] suggested that N_2O is formed over metallic Ag particles. In the present study no significant difference in the amount of N_2O formed over Ag-Al_2O_3 and Ag-ZSM-5 can be seen, indicating that the amount of Ag^0 in these two samples is similar.

In the UV–vis spectra in Fig. 2, the overlapping peaks observed at ca. 230–240 nm for the Ag-ZSM-5 sample and peaks in the region 215–240 nm for the Ag-Al_2O_3 sample are assigned to isolated silver ions [34–39]. Also γ-Al_2O_3 absorbs in this region, however, the absorption for the Ag-Al_2O_3 sample is stronger, why these peaks could be attributed to Ag^+ ions. The absorption in the region 250–260 nm for the Ag-ZSM-5 sample could not be clearly assigned. The Ag-ZSM-5 sample shows absorption in the region 310–330 nm, and the Ag-Al_2O_3 sample has an absorption peak around 350 nm (Fig. 2). Peaks in this region are commonly assigned to small silver clusters ($Ag_n^{\delta+}$) [35–39]. However, the origin of the peak at 300 nm for the Ag-Al_2O_3 sample is not clear. It could be connected to silver clusters or silver aluminate, as suggested by Musi et al. [39]. The presence of metallic silver, expected to absorb in the region 400–420 nm for Ag-ZSM-5 [34–36] and 420–440 nm for Ag-Al_2O_3 [38,39], cannot be clearly established based on the UV–vis spectra

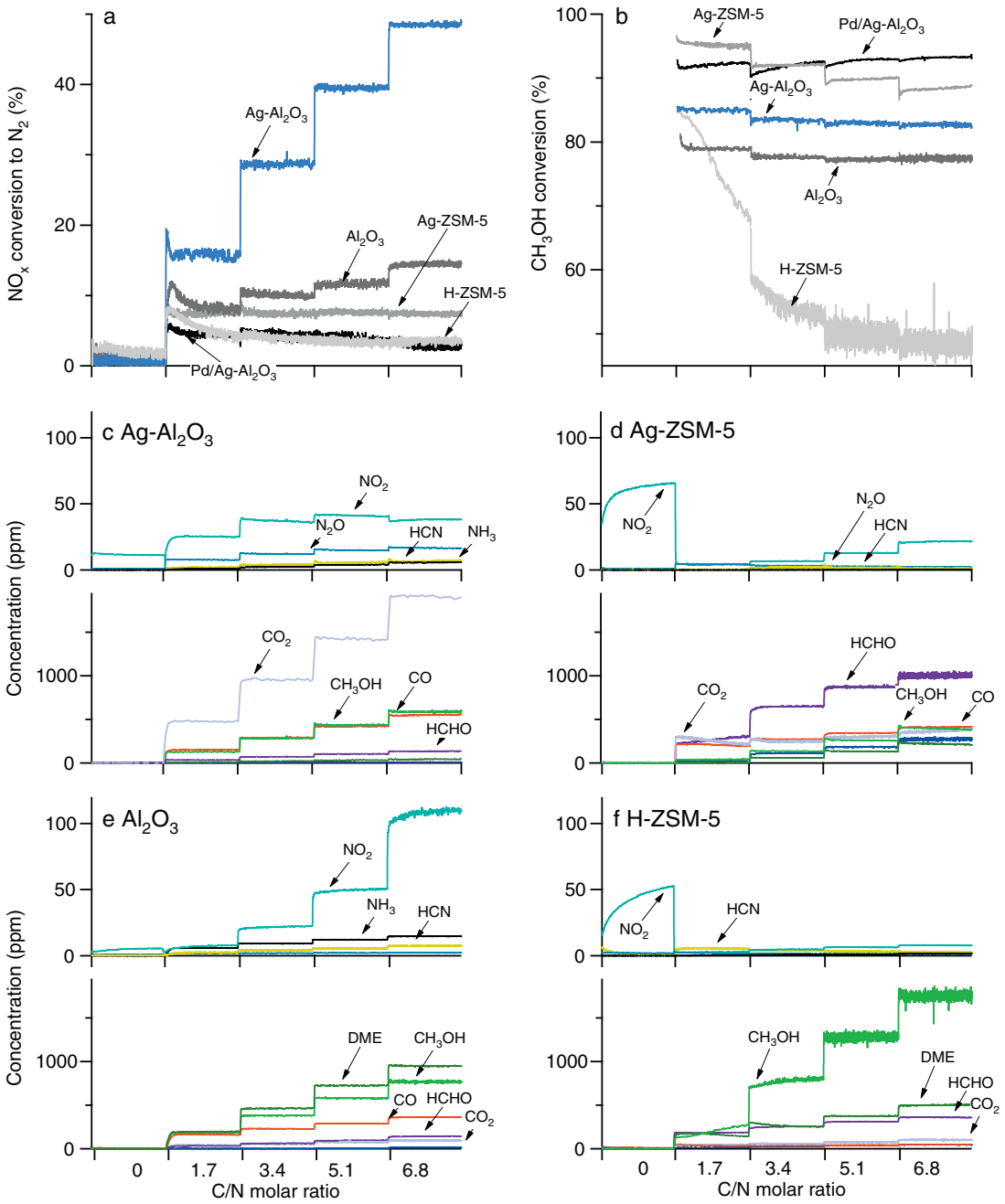

Fig. 6. NO_x conversion to N_2 (a) and methanol conversion (b) over the Al_2O_3, Ag-Al_2O_3, H-ZSM-5, Ag-ZSM-5 and Pd/Ag-ZSM-5 catalysts, and products formed over the (c) Ag-Al_2O_3, (d) Ag-ZSM-5, (e) Al_2O_3 and (f) H-ZSM-5 catalysts, during steady-state experiments at 350 °C in 10% O_2, 500 ppm NO and varying C/N ratio. The upper parts of c–f show the nitrogen containing reaction products, and the lower parts show the carbon containing products and methanol in the outlet flow.

in Fig. 2. Thus, no clear difference between these two samples can be observed based on the UV–vis analysis. The reason behind the difference in NO_x reduction performance could, however, still be related to the nature of the Ag species. Possible explanations are the different ratios between the observed Ag species (the present UV–vis data is not quantitative), or low amounts of Ag species not visible in the UV–vis spectra playing an important role. Another possible reason is that it is an effect of the support material.

4.3. Reaction pathways

In the high temperature region of Fig. 3 complete oxidation to CO_2, occurs over all the tested catalysts, but also CO is formed. Over Ag-Al_2O_3 and Ag-ZSM-5 the formation of CO_2 and CO at lower temperature occurs in the region where NO_x is reduced to N_2, and might thus be a result of the NO_x reduction rather than oxidation by oxygen. The present results are in accordance with those by Wu et al. [9], who observed CO_2 and N_2 as the main products during both methanol and ethanol-SCR over Ag/Al_2O_3. Later a reaction mechanism for NO_x reduction over Ag/Al_2O_3 by C1 reductants where CO_2 was formed together with N_2, was proposed by the same research group [18]. The reaction was suggested to proceed via formate and nitrate species adsorbed on Al sites forming NCO species, which were adsorbed on Ag and Al sites. CO_2 was also suggested to be formed, together with H_2O, from adsorbed formate species. As shown in Fig. 3 CO is formed in the same temperature range as CO_2 over all tested catalysts. CO has been suggested to be formed over Al_2O_3 by decomposition of adsorbed formates [19,30]. More

CO is formed in the high temperature region over Al_2O_3 compared to Ag-Al_2O_3 (Fig. 3), which suggests that CO is formed over active sites on the alumina support at high temperature. The CO observed at lower temperature over Ag-Al_2O_3 might be formed over silver sites.

Formaldehyde is another conversion product detected over all catalysts in this study (Fig. 3), which is likely formed from adsorbed formaldehyde like species as observed by Tamm et al. [19] in DME-SCR over Al_2O_3. For MoO_3 supported on Al_2O_3, intermediates in the NO_x reduction by methanol, discussed by Masters and Chadwick [29], are e.g. adsorbed methoxy groups, followed by adsorbed formyl species, with subsequent formation of formaldehyde. In the present study the formaldehyde detected over the Ag-Al_2O_3 sample indicates a similar reaction mechanism. Over the Ag-ZSM-5 sample, however, even if formaldehyde is the most abundant conversion product from methanol at the temperature for the maximum NO_x conversion, the NO_x reduction is very low (below 5%). Thus, partial oxidation of methanol to formaldehyde is not (an important) part of the NO_x reduction mechanism over Ag-ZSM-5 (and Pd/Ag-ZSM-5). In the lower temperature region of Fig. 3, DME is formed over all the tested catalysts, but to different extent. Over Al_2O_3 high conversion of methanol to DME occurs, likely via adsorbed methoxy groups (—O—CH_3) as suggested by Tamm et al. [19]. The DME formation over the Ag-Al_2O_3 sample is significantly lower than over the Al_2O_3 sample. A possible explanation is that the DME is formed over the Al_2O_3 support rather than over Ag sites. Fig. 3 shows that the DME formation mainly occurs at lower temperatures than the NO_x conversion. From this, and the fact that the conversion of methanol to DME is not an oxidation reaction, we conclude that the formation of DME is not part of the NO_x reduction mechanism.

4.4. Influence of hydrogen

A way of promoting the SCR activity at low temperatures over supported Ag catalysts, and especially Ag-Al_2O_3, is to utilize the positive effect of H_2 addition [40,41]. Despite several suggestions in the literature the mechanism of the promoting effect of H_2 addition is not yet fully understood. Fig. 4 shows a positive influence of H_2 over all Ag containing samples. Addition of hydrogen results in broader temperature interval of NO_x reduction towards lower temperatures and increased NO_x reduction. The most pronounced effect is seen over Ag-Al_2O_3, while the NO_x reduction over the two ZSM-5 based catalysts remains low even in the presence of H_2 (Fig. 4). This is in agreement with the study by Konova et al. [42], who reported that the NO_x conversion over Ag(2.7%)-ZSM-5 in octane-SCR was essentially lower than over Ag(2%)-Al_2O_3, even in the presence of H_2. In propene-SCR over Ag-ZSM-5, the introduction of H_2, in fact, resulted in lower NO_x reduction [42]. Thus, hydrogen seems not to enhance the NO_x reduction significantly over Ag-ZSM-5, at these silver loadings (ca. 3–5%). Over Ag-Al_2O_3, however, the presence of hydrogen does influence the NO_x reduction and shifts the formation of all detected species towards lower temperatures, shown in Fig. 5. When H_2 is present more N_2, NO_2 and N_2O are formed. The increased formation of NO_2 in the presence of H_2 is in accordance with the observations by Breen et al. [43] who reported that NO_2 formation plays an important role in the H_2 assisted SCR over Ag/Al_2O_3 at low H_2 concentrations (500 and 1000 ppm). Fig. 5 shows that methanol conversion over Ag-Al_2O_3 starts at lower temperatures in the presence of H_2 and in particular more CO_2 is formed, while the formation of DME and CO (at high temperatures) decreases. During the whole temperature interval where NO_x is reduced to N_2 the conversion products from methanol are oxidized to a higher extent, see the bottom panel of Fig. 5. This is in accordance with recent findings by Shimizu et al. [44] who reported that one of the main roles of hydrogen in H_2 assisted HC-SCR is to enhance partial oxidation of hydrocarbons to surface oxygenates. This is suggested to proceed via formation of H_2O_2-like active oxygen species, formed over Ag-hydride clusters. The experiments with increasing C/N molar ratio (Fig. 6), on the other hand, results in a constant ratio between the concentration of each carbon containing product and the supplied methanol when the methanol concentration is increased. As this is different from when hydrogen is introduced to the feed and more oxidized carbon species are formed, it implies that hydrogen does not act as a reducing agent.

To our knowledge there are no previous studies in the open literature regarding the effect of H_2 on methanol-SCR. However, for ethanol-SCR a promotional effect by H_2 has been reported by Zhang et al. [45] and da Silva et al. [3]. Zhang et al. [45] reported that H_2 promotes the partial oxidation of ethanol to enolic species, which readily react with adsorbed nitrates and contribute to the NO_x reduction. H_2 also promotes the formation of NH_x species, possibly via hydrolysis of —NCO by formed —OH groups. The NH_x species are known to be active in the NO_x reduction by NH_3. Da Silva et al. [3] reported that the main promotional effect of hydrogen addition on ethanol-SCR is the promotion of partial oxidation of ethanol to acetaldehyde. Detection of acetaldehyde in the outlet flow is also an indication of the presence of enolic species (RCH=CH—O), which result in high efficiency for ethanol-SCR in their reaction with nitrate species, in studies by Yu et al. [5]. For propene-SCR da Silva et al. [3] proposed that the main promoting effect of H_2 is via the formation of metallic silver nano-agglomerates, which would enhance the NO_x reduction by activation of the reducing agent. Considering the insignificant amounts of acetaldehyde formed in the present study, the NO_x reduction route via enolic species does not explain the positive effect of H_2 on methanol-SCR. However, more NO is oxidized to NO_2, and more methanol is partially oxidized to formaldehyde on the expense of the formation of DME over Ag-Al_2O_3 (Fig. 5) when H_2 is added to the flow. Since NO_2 is known to be more active in SCR reactions than NO, the higher formation of NO_2 can be an explanation of the positive effect caused by H_2. However, also the increase in the formaldehyde formation can be part of the H_2 effect, even if it can be questioned since the high formation of formaldehyde over Ag-ZSM-5 (Fig. 3) did not result in any considerable reduction of NO_x. He et al. [18] suggested that NCO species are part of the NO_x reduction mechanism for C1 reductants. This opens for the possibility of H_2 promoting NO_x reduction by methanol via formation of NH_x species and hydrolysis of surface isocyanates as suggested by Zhang et al. [45] for ethanol-SCR. Da Silva et al. [3] claimed that the increase of N_2O in the outlet flow when H_2 is added is an indication of the formation of small metallic Ag clusters. Also in the present study the formation of N_2O increases when H_2 is added to the flow, however, not extensively (Fig. 5). Kannisto et al. [41] did, on the other hand, not detect any reduction of silver species when Ag-Al_2O_3 was exposed to H_2. Reduction of surface nitrates was, however, observed and suggested to be important for the H_2 effect.

4.5. The C/N molar ratio

To further investigate possibilities to improve the NO_x reduction performance steady-state (at 350 °C) experiments with increasing methanol concentration, i.e. increasing the C/N molar ratio of the reactants, were performed. Tabata et al. [17] reported enhanced NO_x reduction over Al_2O_3 in methanol-SCR at 400 °C, both with increasing methanol concentration while keeping the NO concentration constant, and with decreasing NO concentration while keeping the C/N ratio constant. Fig. 6 shows that the NO_x reduction at 350 °C over Ag-Al_2O_3 can be improved by increasing the methanol content in the feed gas. The selectivity to N_2 increases, but also the concentration of unwanted by-products (N_2O, NH_3 and HCN). A positive effect can be seen also over the Al_2O_3 sample, while

the NO_x reduction over the ZSM-5 based samples is not influenced by an increase in the C/N molar ratio. For Al_2O_3 and H-ZSM-5, it is worth noting that the low impact of increasing the C/N molar ratio could be due to the temperature (350 °C) being considerably lower than the temperature for the maximum NO_x conversion seen in the temperature ramp experiments. However, since we focus on temperatures typical for lean burn applications (200–350 °C), no experiments with varying C/N molar ratio were performed at higher temperatures. On the contrary to when hydrogen is introduced to the feed and more oxidized carbon species are formed over Ag-Al_2O_3, the ratio between the concentration of each carbon containing product and the inlet methanol remains constant when the methanol concentration is increased. H-ZSM-5, in contrast to the other samples, shows a significant decrease in methanol conversion with increasing C/N ratio (Fig. 6). This could be due to poisoning of the catalyst surface by carbon, since H-ZSM-5 is the sample that is least active for methanol oxidation at the tested temperature (350 °C). As an increase of the methanol concentration over the Al_2O_3 based samples increases the NO_x reduction, we conclude that the reducing agent is a limiting factor for the NO_x reduction in the cooling ramp experiments at the C/N molar ratio 1.7. Thus, the amount of active sites on the Al_2O_3 based catalysts seems not to be a limiting factor in the reaction conditions in the present study, which suggests that the NO_x reduction performance over the Al_2O_3 based samples could be improved even further by optimizing the reaction conditions. However, there are two major disadvantages with increasing the methanol content in the feed. One is the higher methanol slip and increased formation of unwanted by-products. For Ag-Al_2O_3 the most abundant species in the outlet flow are methanol, CO and HCHO. In a real application these could possibly be handled by an oxidation catalyst. Another drawback with increasing the C/N molar ratio is the higher fuel penalty. Kannisto et al. [46] reported for HC-SCR with diesel as reducing agent, that a C/N molar ratio of 6–8 and a H_2 addition of 1000 ppm (which correspond to conditions in the present work), give a fuel penalty of 2%. For comparison the authors pointed out that the cost for urea-SCR is equivalent to a (diesel) fuel penalty of ca. 0.5%. Thus, it is important to keep the consumption of both reducing agent and hydrogen low.

5. Concluding remarks

In order to achieve a good NO_x reduction performance in methanol-SCR a catalytic material which gives a low level of combustion of the reducing agent is essential. The support material, the preparation method (the sol–gel method using freeze-drying) and the low Ag loading (2 wt%) are suggested to be important factors for the Ag-Al_2O_3 sample giving relatively high NO_x reduction.

The NO_x reduction over Ag-Al_2O_3 with methanol is proposed to occur by adsorbed nitrates or nitrites (or gas phase NO_2) reacting with adsorbed acetate or formaldehyde like species forming adsorbed R—NO_2 or R—ONO, with subsequent conversion into —NCO, —CN, R—NH_2 or NH_3, with final desorption of N_2 and CO_x (or HCHO). The formation of DME, possibly via adsorbed methoxy groups, is suggested not to be part of the NO_x reduction mechanism. The hydrogen effect, known to promote NO_x reduction at low temperatures over supported Ag catalysts, was also studied. Especially for Ag-Al_2O_3, the results show that H_2 addition broadens the active temperature interval towards lower temperatures and increases the maximum NO_x reduction. The addition of hydrogen to the feed was also observed to result in formation of more oxidized carbon species. The NO_x reduction over Ag-Al_2O_3 was significantly improved by increasing the methanol content in the feed gas, however, on the expense of higher fuel penalty. A positive effect was seen also over Al_2O_3, while the NO_x reduction over the ZSM-5 based samples was unaffected.

The Ag-Al_2O_3 catalyst prepared by the sol–gel method, including freeze-drying of the formed gel, is concluded to be the most promising candidate of the tested catalysts for methanol-SCR. Its performance can be improved by optimizing the C/N molar ratio and, especially at low temperatures, by including H_2 in the gas feed. The support material, the Ag loading and the nature of the Ag sites are suggested to play important roles in the NO_x reduction over supported Ag catalysts.

Acknowledgments

This work has been funded by the Swedish Energy Agency and performed within the Competence Centre for Catalysis, which is hosted by Chalmers University of Technology and financially supported by the Swedish Energy Agency and the member companies: AB Volvo, ECAPS AB, Haldor Topsøe A/S, Saab Automobile Powertrain AB, Scania CV AB and Volvo Car Corporation AB. Financial support from Knut and Alice Wallenberg Foundation, Dnr KAW 2005.0055, and Chalmers Area of Advance Transport are gratefully acknowledged.

References

[1] S. Roy, M.S. Hegde, G. Madras, Appl. Energy 86 (2009) 2283–2297.
[2] K. Shimizu, A. Satsuma, T. Hattori, Appl. Catal. B 25 (2000) 239–247.
[3] R. da Silva, R. Cataluna, A. Martinez-Arias, Catal. Today 143 (2009) 242–246.
[4] C.B. Zhang, H. He, S.J. Shuai, J.X. Wang, Environ. Pollut. 147 (2007) 415–421.
[5] Y.B. Yu, H. He, Q.C. Feng, H.W. Gao, X. Yang, Appl. Catal. B 49 (2004) 159–171.
[6] A. Abe, N. Aoyama, S. Sumiya, N. Kakuta, K. Yoshida, Catal. Lett. 51 (1998) 5–9.
[7] S. Sumiya, M. Saito, H. He, Q.C. Feng, N. Takezawa, K. Yoshida, Catal. Lett. 50 (1998) 87–91.
[8] T. Miyadera, Appl. Catal. B 2 (1993) 199–205.
[9] Q. Wu, H. He, Y.B. Yu, Appl. Catal. B 61 (2005) 107–113.
[10] S. Kameoka, Y. Ukisu, T. Miyadera, Phys. Chem. Chem. Phys. 2 (2000) 367–372.
[11] S. Tamm, H.H. Ingelsten, M. Skoglundh, A.E.C. Palmqvist, Top. Catal. 52 (2009) 1813–1816.
[12] K. Masuda, K. Tsujimura, K. Shinoda, T. Kato, Appl. Catal. B 8 (1996) 33–40.
[13] T.L. Zhu, R.M. Hao, L.X. Fu, J.H. Li, Z.M. Liu, React. Kinet. Mech. Catal. 84 (2005) 61–67.
[14] R. Burch, E. Halpin, J.A. Sullivan, Appl. Catal. B 17 (1998) 115–129.
[15] F.C. Meunier, R. Ukropec, C. Stapleton, J.R.H. Ross, Appl. Catal. B 30 (2001) 163–172.
[16] H. Kannisto, H.H. Ingelsten, M. Skoglundh, J. Mol. Catal. A: Chem. 302 (2009) 86–96.
[17] M. Tabata, H. Tsuchida, K. Miyamoto, T. Yoshinari, H. Yamazaki, H. Hamada, Y. Kintaichi, M. Sasaki, T. Ito, Appl. Catal. B 6 (1995) 169–183.
[18] H. He, X.L. Zhang, Q. Wu, C.B. Zhang, Y.B. Yu, Catal. Surv. Asia 12 (2008) 38–55.
[19] S. Tamm, H.H. Ingelsten, M. Skoglundh, A.E.C. Palmqvist, J. Catal. 276 (2010) 402–411.
[20] S. Tamm, H.H. Ingelsten, A.E.C. Palmqvist, J. Catal. 255 (2008) 304–312.
[21] K. Masuda, K. Shinoda, T. Kato, K. Tsujimura, Appl. Catal. B 15 (1998) 29–35.
[22] H.H. Ingelsten, D.M. Zhao, A. Palmqvist, M. Skoglundh, J. Catal. 232 (2005) 68–79.
[23] I. Chorkendorff, J.W. Niemantsverdriet, Concepts of Modern Catalysis and Kinetics, Wiley-VCH GmbH & Co. KGaA, 2003, pp. 185–190.
[24] C. Wang-Hansen, C.J. Kamp, M. Skoglundh, B. Andersson, P.-A. Carlsson, J. Phys. Chem. C 115 (2011) 16098–16108.
[25] M.W. Ngobeni, A.F. Carley, M.S. Scurrell, C.R. Nicolaides, J. Mol. Catal. A: Chem. 305 (2009) 40–46.
[26] M. Iwasaki, K. Yamazaki, K. Banno, H. Shinjoh, J. Catal. 260 (2008) 205–216.
[27] P. Lersch, F. Bandermann, Appl. Catal. 75 (1991) 133–152.
[28] E.M. Cordi, J.L. Falconer, Appl. Catal. A 151 (1997) 179–191.
[29] S.G. Masters, D. Chadwick, Appl. Catal. B 23 (1999) 235–246.
[30] A.R. McInroy, D.T. Lundie, J.M. Winfield, C.C. Dudman, P. Jones, D. Lennon, Langmuir 21 (2005) 11092–11098.
[31] S. Tamm, H.H. Ingelsten, A.E.C. Palmqvist, Catal. Lett. 123 (2008) 233–238.
[32] K.A. Bethke, H.H. Kung, J. Catal. 172 (1997) 93–102.
[33] F.C. Meunier, J.P. Breen, V. Zuzaniuk, M. Olsson, J.R.H. Ross, J. Catal. 187 (1999) 493–505.
[34] S.J. Miao, Y. Wang, D. Ma, Q.J. Zhu, S.T. Zhou, L.L. Su, D.L. Tan, X.H. Bao, J. Phys. Chem. B 108 (2004) 17866–17871.
[35] C. Shi, M.J. Cheng, Z.P. Qu, X.H. Bao, Appl. Catal. B 51 (2004) 171–181.
[36] P. Sazama, H. Jirglova, J. Dedecek, Mater. Lett. 62 (2008) 4239–4241.
[37] K. Arve, L. Capek, F. Klingstedt, K. Eranen, L.E. Lindfors, D.Y. Murzin, J. Dedecek, Z. Sobalik, B. Wichterlova, Top. Catal. 30 (1) (2004) 91–95.
[38] X. She, M. Flytzani-Stephanopoulos, J. Catal. 237 (2006) 79–93.

[39] A. Musi, P. Massiani, D. Brouri, J.M. Trichard, P. Da Costa, Catal. Lett. 128 (2009) 25–30.
[40] J.P. Breen, R. Burch, Top. Catal. 39 (2006) 53–58.
[41] H. Kannisto, H.H. Ingelsten, M. Skoglundh, Top. Catal. 52 (2009) 1817–1820.
[42] P. Konova, K. Arve, F. Klingstedt, P. Nikolov, A. Naydenov, N. Kumar, D.Y. Murzin, Appl. Catal. B 70 (2007) 138–145.
[43] J.P. Breen, R. Burch, C. Hardacre, C.J. Hill, C. Rioche, J. Catal. 246 (2007) 1–9.
[44] K. Shimizu, K. Sawabe, A. Satsuma, Catal. Sci. Technol. 1 (2011) 331–341.
[45] X.L. Zhang, H. He, Z.C. Ma, Catal. Commun. 8 (2007) 187–192.
[46] H. Kannisto, X. Karatzas, J. Edvardsson, L.J. Pettersson, H.H. Ingelsten, Appl. Catal. B 104 (2011) 74–83.